

Performance-based viscous force field adaptation in upper limb strength training for stroke patients

Conference Paper**Author(s):**

Baur, Kilian ; Klamroth-Marganska, Verena ; Giorgetti, Chiara; Fichmann, Daniela; Riener, Robert

Publication date:

2016

Permanent link:

<https://doi.org/10.3929/ethz-b-000119887>

Rights / license:

[In Copyright - Non-Commercial Use Permitted](#)

Originally published in:

<https://doi.org/10.1109/BIOROB.2016.7523736>

Performance-based viscous force field adaptation in upper limb strength training for stroke patients

Kilian Baur^{*†}, Verena Klamroth-Marganska^{*†}, Chiara Giorgetti, Daniela Fichmann, Robert Riener^{*†}

^{*} Sensory-Motor Systems Lab, ETH Zurich, Switzerland

[†] University Hospital Balgrist, University of Zurich, Switzerland

Abstract—Muscle weakness is one of the major deficits after stroke but specific strength training is seldom included in robot-assisted rehabilitation. At the same time, the emergence of robotic devices for stroke therapy offers technical possibilities for strength training. We propose a control strategy for strength training that is based on a viscous force field shaped towards the patient's performance abilities at different positions and directions during a movement. The controller was implemented in the arm rehabilitation robot ARMin in combination with a one-degree-of-freedom repetitive tracking task. The viscous force field is adapted in each round as a function of the local performance profile (shape) and the performance sum of each round (task level). The patient gets feedback by visual representation of the tracking task displaying the position of the moving target object and the position of the patient cursor. We hypothesize that the performance-shaped task level of the viscous force field demands the maximum effort of the participant at each point of the trajectory. Furthermore, we hypothesize that the participants are more motivated by this controller for strength training than by controllers using a constant task level. The controller was tested in a feasibility study with 31 healthy subjects. The resulting individual task level of the viscous force field increased compared to the initial state but did not reach a steady state by (visual inspection). No differences in motivation compared to a controller using a constant viscous force field were identified. We propose the framework of differentiation in shape and task level of a viscous force field for difficulty adaptation in future rehabilitation games.

I. INTRODUCTION

Muscle strength is considered as crucial for performance of tasks of daily living [1]. Muscle weakness is one of the major deficits after stroke [2] and may be substantially contributing to compromised functional performance [1]. Literature implies that specific strength training may yield to higher gains in muscle strength than conventional rehabilitation therapy and improve motor function [3].

In the past, specific strength training was not included in rehabilitation processes, mainly due to the assumption that it increased spasticity and abnormal motor function [4], [5]. Recent studies showed significant improvements in upper and lower limbs strengths in stroke survivors after resistance training without increase in spasticity or abnormal motor function [3], [6], [7]. Motor patterns in patients observed following resistance training were more similar to those of healthy subjects as compared to those in patients assigned to functional task practice [8].

The emergence of robotic devices for stroke therapy offers control strategies for an individually customized

strength training [9], [10]. Several control strategies with performance-based adaptation of task parameters have been presented in literature. Performance-based adaptation was also considering position and direction dependent performance of the patient to learn a time-based model of forces in a reaching task [11]. However, most existing control strategies apply a constant resistive force or a constant viscous field to the patient [12], [13]. Such control strategies consider neither the position, velocity and direction dependencies of the individual strength nor the variability of the physical abilities between stroke patients [14], [15]. Both, kinematic dependency of individual strength and inter-patient variability claim for customizable task difficulties in strength training after stroke [16].

We developed a new control approach for robot-assisted therapy. An adaptive viscous force field enables a customized strength training for stroke patients considering the individual strength profile. The control design was tested in a feasibility study.

II. CONCEPT

A. Task and control design

The control design is based on an adaptive viscous force field in a repetitive tracking task. The adaptation of the profile derives from the individual performance within the tracking task. The adaptation is applied not only at the general level (i.e., task level) considering inter-patient variability in strength. It also accounts for the kinematic dependency of strength of the individual patient by shaping the viscous force field within the trajectory, as a function of location and direction of the target object.

B. General control concept

The target object C_T moves from the start point (transition point) P_S along the trajectory back to the start point P_S within the period T (Figure 1). This trajectory is represented by the position of the target object at a specific normalized time s .

$$s = \frac{t}{T}, 0 \leq t \leq T \quad (1)$$

$$t_{P_s} = 0, st_{P_s} = 0 \quad (2)$$

One round or repetition of the task is defined as the target trajectory starting and ending at P_S , and the round index i is

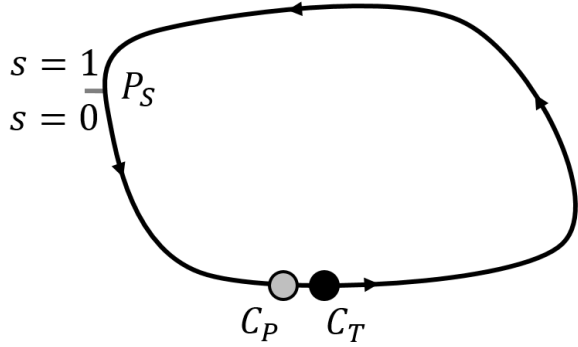


Fig. 1. Task design in a two-degree-of-freedom example. The flashes represent the movement direction. The patient moves the cursor C_P (grey dot) trying to track the target object C_T (black dot). The control variable s (normalized time) starts at P_S with $s = 0$.

increasing incrementally by 1 whenever C_T is passing P_S . During the first round the index i is 1. In each round s is starting from 0.

Throughout each round three profiles define task difficulty and performance of the patient:

- velocity profile $v_i(s)$
- viscous force field $r_i(s)$
- performance profile $p_i(s)$

The predefined velocity profile $v_i(s)$ refers to the movement of the target object C_T . It does not change between the rounds (i.e. $v_i(s) = v(s)$). The participant is instructed to track C_T during the entire task and moves the cursor C_P with velocity $\dot{x}_P(s)$.

A viscous force field $r_i(s)$ is applied and challenges the participant in keeping track of C_T . The initial viscous force field, used in the first round, is the predefined viscous force field $r_1(s)$. The viscous force field changes over time and generates velocity dependent forces that (in case of positive viscosity) counteract to the movement and thus require force from the participant. The performance profile $p_i(s)$ can be indicated by any quality of movement measure that can give an immediate performance measure at any value of s (e.g. position error, velocity error).

$$p_i(s) = p_i(x_P(s), \dot{x}_P(s)) \quad (3)$$

The viscous force field is updated according to the performance during the previous round.

$$r_{i+1} = r_{i+1}(r_i, p_i) \quad (4)$$

We propose two separate update sections (Figure 2) :

(1) shape update

The viscous force field is shaped based on the normalized local performance values $\tilde{r}_{i+1}(s)$, scaled and converted into viscous force field by the factor c_1 . It is represented by the shape of the viscous force field along the track.

(2) task level update

The general task level \bar{r}_i (mean level of the viscous force field) is set according to the overall performance \bar{p}_i of one entire round, scaled and converted to the resistance space by the factor c_2 .

Both update sections are added to the viscous force field of the previous round reduced by a forgetting factor $(1 - L)$:

$$\hat{r}_{i+1} = (1 - L)r_i(s) + Lc_1\tilde{r}_{i+1}(s) + c_2\bar{p}_i \quad (5)$$

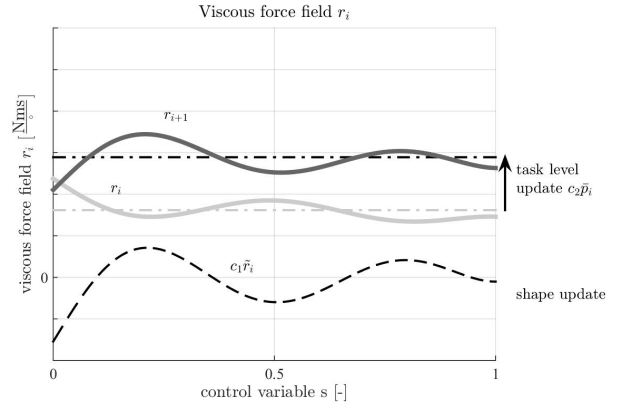


Fig. 2. The update of the viscous force field profile is separated into a shape of level section and a task level section. The shape of level defines difference in the viscous force field according to local abilities of the patient regarding the task execution. The task level defines the general level of the viscous force field regarding the task execution.

For the two update sections we propose the following functions:

(1) shape update

$$\tilde{r}_{i+1}(s) = p_{i,N}(s) = \frac{p_i(s) - p_{i,min}}{p_{i,max} - p_{i,min}} \quad (6)$$

(2) task level update

$$\bar{p}_i = f(p_{i,\Sigma}) = f\left(\int_{s=0}^1 p_i(s) ds\right) \quad (7)$$

Since this round based update will end up in a discontinuous behavior at the transition point P_S , transition conditions shall force the viscous force field to be continuous during the transition phase.

$$\hat{r}_{i+1}(s=0) = \hat{r}_i(s=1) \quad (8)$$

$$\hat{r}'_{i+1}(s=0) = \hat{r}'_i(s=1) \quad (9)$$

To reduce the number of data points stored during the task and to smooth the profile, the viscous force field is reduced to a polynomial regressed function. The data points from both the shape section and the transition conditions are used as an input for the polynomial regression of order n .

$$r_{i+1} = p_n(\hat{r}_{i+1}, r_i(1), r'_i(1)) \quad (10)$$

C. Feasibility study

1) *Device*: The task was implemented into the therapy robot ARMin IV which, through its exoskeleton structure, allows not only for measurement of kinematic- and time-based, but also for kinetic-based parameters (Figure 3).



Fig. 3. Subject using the ARMin arm robot. The visual display is used to present task visualization.

The arm therapy robot ARMin has been designed and evaluated by the groups of Riener and Dietz/Curt at ETH Zurich and University of Zurich [17], [18], respectively. ARMin is used for the therapy of the arm of neurological patients. The latest generation has seven degrees of freedom (DOF) allowing 3D shoulder rotation, elbow flexion/extension, pro-/supination and wrist flexion/extension. A hand actuation module supports and measures opening and closing of the hand [19]. The ARMin exoskeleton is connected with the human arm with cuffs located at the upper arm, the lower arm and the fingers. The newest prototype of the ARMin robot (i.e., ARMin IV) is equipped with six-degrees of freedom force sensors placed on each cuff. These force sensors measure the interaction forces between the patient and the robot itself [20].

ARMin can be adjusted to the patient by changing the exoskeleton length settings for the upper arm, the forearm and the hand as well as the shoulder height. The same robot can be used for the training of the left and right arm by changing the hardware configuration. Mechanical end limits are provided for safety reasons to not overstretch joints or collide with the patient. The ARMin robot features different control modes covering continuously the range from a compensation only setting, where the robot's weight and friction are compensated, to complete guidance of the arm. ARMin is particularly useful to assess kinetic and kinematic arm functions on single joint and end-effector levels. ARMin is controlled with Simulink Realtime (Mathworks, R2014b).

D. Task design

The trajectory selected for the feasibility study was a one-DOF movement in elbow flexion-extension with constant speed. The tracking task was represented in a visualization of the target object and the patient cursor programmed in Unity 3D (Unity Technologies, 5.1) (Figure 4).

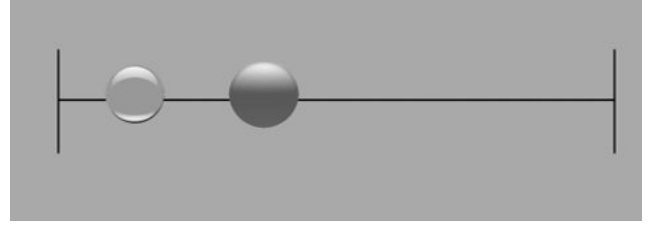


Fig. 4. Task visualization. The target object (dark grey) follows the one-DOF trajectory starting from the left edge and moving with constant velocity to the right edge and back. The patient moves the patient cursor (light grey) to track the target object.

Summary of task parameters:

- Period of trajectory $T = 18$ s
- Trajectory length 180° (90° elbow extension, 90° elbow flexion)
- velocity profile $v = 10^\circ/\text{s}$

The task was performed for five minutes resulting in a total number of 16 completed rounds. The controller started initially with minimal viscous forces where only friction and inertia effects were felt by the participant. The performance was measured as the position error $e_{x,i}(s)$ between target object and patient cursor. Summary of control parameters:

- initial viscous force field $r_1(s) = 0$ Nms/ $^\circ$
- performance measure $p_i(s) = \frac{1}{e_{x,i}(s)} = \frac{1}{|x_{t,i}(s) - x_{p,i}(s)|}$
- update of viscous force field

(1) shape update

$$\tilde{r}_{i+1}(s) = (0.5 - p_{i,N}(s)) \quad (11)$$

(2) task level update

$$p_{i,\Sigma} = \int_{s=0}^1 \frac{1}{e_{x,i}(s)} ds \quad (12)$$

$$\bar{p}_i = \begin{cases} -0.1 & p_{i,\Sigma} < 0.3/^\circ \\ 0.4 & p_{i,\Sigma} > 0.45/^\circ \\ (-1.1 + \frac{10^\circ}{3} p_{i,\Sigma}) & \text{otherwise} \end{cases} \quad (13)$$

- learning rate $L = 0.5$
- scaling factors $c_1, c_2 = 1$ Nms/ $^\circ$

The range of $0.30/^\circ$ to $0.45/^\circ$ was defined experimentally as a convenient performance range for healthy subjects. The task level step sizes of -0.1 and 0.4 were selected to enable a fast increase of the viscous force field towards an individual maximum profile with option to reduce the viscous force field with decreasing performance.

The polynomial regression was performed at an order of ten. This equals the highest possible order that was possible from a technical point of view and therefore, represents the performance of the patient with best accuracy.

$$r_{i+1} = p_{10}(\hat{r}_{i+1}, r_i(1), r'(1)) \quad (14)$$

A validation or optimization of the polynomial order was not part of this project. For this first implementation the viscous forces were restricted to a minimum of 0 Nms/ $^\circ$.

TABLE I
INCLUSION CRITERIA

Inclusion criteria
<ul style="list-style-type: none"> • Minimum age of 18 years • Bodyweight under 120 kg • No excessive spasticity of the affected arm ($mAS < 4$) • No serious medical or psychiatric disorder as reported by the participant • No orthopaedic, rheumatic or other disease restricting movements of the paretic arm • No shoulder subluxation of more than two fingers width • No skin ulcerations of the paretic arm • Ability to communicate appropriately with the examiner so that the validity of the patient's data is not compromised • No cyber sickness • No pacemaker or other implanted electronic device • No serious cognitive deficiency or aphasia preventing from appropriate use of ARMin

E. Study design

The control design was tested in a feasibility study with 31 healthy subjects (16 female, average age $32.1 (\pm 14.7)$ years, all right handed as stated by participants) from June 22, 2015 to August 26, 2015. Subjects were recruited through the social network of lab members. They were eligible if they met inclusion criteria (Table I). They all used their dominant (i.e. right) arm.

We hypothesized that the controller would shape the viscous force field towards a maximum task level. The individual task level maximum was identified by a visual evaluation of the changes of the viscous force field between different rounds of the repetitive tracking task.

Secondarily, we hypothesized that due to the adaptive viscous force field the motivation of the participants was increased compared to a design without an adaptive viscous force field. The motivation was measured with the Intrinsic Motivation Inventory (IMI) [21]. The IMI has previously been used with virtual environments for motor rehabilitation [22], [23], [24]. It consists of sixteen selected statements divided into four scales: interest/enjoyment, perceived competence, effort/importance and value/usefulness. Subjects rate how true each statement is on a 7-point scale, with 1 indicating “not at all true”, and 7 indicating “very true”. The mean values of each subject for the two game modes were considered for the evaluation. The possible range for each score was therefore 1-7. The game mode without an adaptive viscous force field included the same visual task design but with a constant viscous force field $r_i = 0.5 \text{ Nms}/^\circ$. The two game modes were performed in randomized order.

III. RESULTS

Twenty-nine out of 31 participants completed the task. Representative data of one participant is presented in Figure 5. The viscous force field increased between first and last round in all participants. None of the participants reached a plateau during the total 16 rounds by visual interpretation of the mean viscosity (Figure 6 and Figure 7).

The subjects rated the strength training with viscous force field adaptation as diversified and more challenging (perceived competence) compared to the training with constant

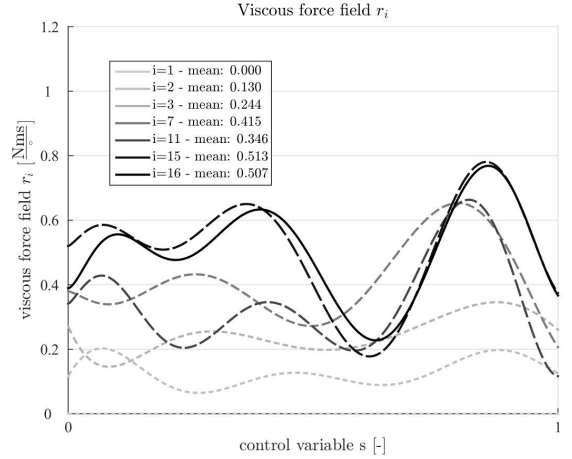


Fig. 5. Progress of the viscous force field of one individual participant. The viscous force field was not only shaped towards the local abilities of the patient (i.e., shape of each curve) but also with increasing global level of the viscous force field (relative position of each curve).

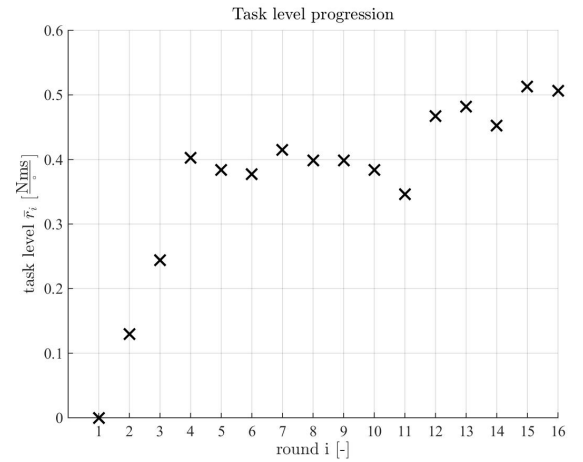


Fig. 6. Progress of the task level (mean level of the viscous force field) of one individual subject. The task level increases not monotonous. A trend towards a plateau can be indicated but no steady-state level be identified.

viscous force field. However, they did not evaluate the strength training with viscous force field adaptation as more motivating (Figure 8).

IV. DISCUSSION AND OUTLOOK

We could successfully implement a new control approach for robot-assisted therapy. The controller could increase the level of the viscous force field (i.e. the task level) towards the maximum of a healthy subject and adjusted the shape of the task level according to the individual strength of the subject.

The time duration selected for the task in the feasibility study was not sufficient to force the patient to reach a plateau. Therefore we claim for longer task duration to identify the individual maximum. The term for the actual round of the update function includes not only the shape but also the task level from the previous round. We propose a separation of

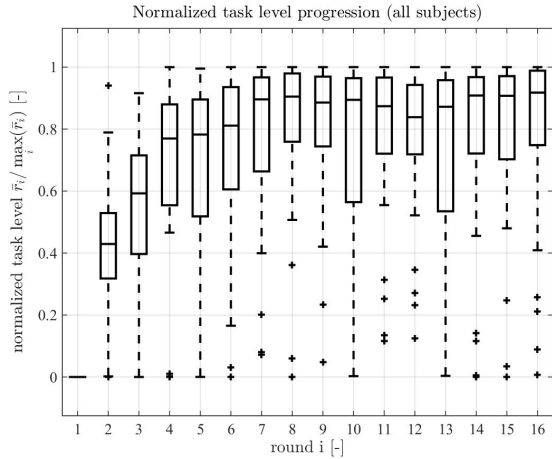


Fig. 7. Progress of the normalized task level (mean level of the viscous force field) of subjects. The task level was normalized by the maximum task level over all rounds. Despite a high variability over all subjects a trend towards a plateau can also be indicated within all subject group.

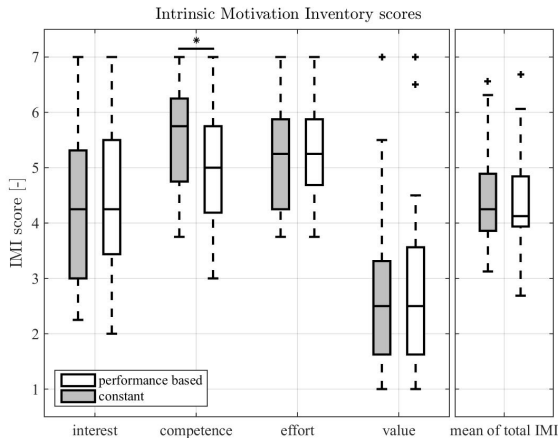


Fig. 8. IMI scores in all four subscales and the mean of the total IMI, for the two game modes: constant viscous force fields (white) and performance-based update of the viscous force field (grey). No significant difference in the subscales interest/enjoyment ($p = 0.36$), effort/importance ($p = 0.12$) and value/usefulness ($p = 0.23$) between the two game modes can be observed. Significant difference in the subscale perceived competence ($p < 0.001$). No significant difference in the mean value of the IMI subscales ($p = 0.41$).

these two elements for further applications to clearly separate the two update sections. In later rounds the normalization caused a disproportional influence of the error. Therefore, the normalization of the error for the shaping shall be replaced by a scaling of the error.

The selected velocity profile of the task leads to high positions errors at the positions where the tracking cursor changes direction due to infinite accelerations. For a future task design we propose finite accelerations that can be performed by patients, e.g. sinusoidal velocity profiles for one-DOF tracking tasks.

The restriction of the viscous force field to a minimum of 0 Nms° could be abolished to enable supporting forces fields for disabled participants. This has to be tested with

stroke patients after a redesign of the update method.

V. CONCLUSIONS

The successful implementation of a performance-based strength training using an adaptation of a viscous force field showed great potential to enhance the outcome regarding strength and function in robot-assisted rehabilitation. The results of the feasibility study will be used for a redesign of the implemented controller and to prepare a study design considering healthy and disabled participants.

ACKNOWLEDGMENT

This work was supported by the Swiss National Science Foundation (Grant No. SNF-106313) through the National Centre of Competence in Research on Robotics (NCCR) and by the ETH Foundation through ETH Research Grant ETH-17 13-2.

REFERENCES

- [1] C. Patten, J. Lexell, and H. E. Brown, "Weakness and strength training in persons with poststroke hemiplegia: rationale, method, and efficacy," *Journal of rehabilitation research and development*, vol. 41, no. 3A, pp. 293–312, 2004.
- [2] R. Bohannon, "Muscle strength and muscle training after stroke," *Journal of Rehabilitation Medicine*, vol. 39, no. 1, pp. 14–20, 2007.
- [3] L. Ada, S. Dorsch, and C. G. Canning, "Strengthening interventions increase strength and improve activity after stroke: a systematic review," *The Australian journal of physiotherapy*, vol. 52, no. 4, pp. 241–8, 2006.
- [4] G. J. Miller and K. E. Light, "Strength training in spastic hemiparesis: should it be avoided?," *NeuroRehabilitation*, vol. 9, no. 1, pp. 17–28, 1997.
- [5] G. T. Thielman, C. M. Dean, and a.M. Gentile, "Rehabilitation of reaching after stroke: Task-related training versus progressive resistive exercise," *Archives of Physical Medicine and Rehabilitation*, vol. 85, pp. 1613–1618, oct 2004.
- [6] U. B. Flansbjerg, M. Miller, D. Downham, and J. Lexell, "Progressive resistance training after stroke: Effects on muscle strength, muscle tone, gait performance and perceived participation," *Journal of Rehabilitation Medicine*, vol. 40, no. 1, pp. 42–48, 2008.
- [7] M. M. Ouellette, N. K. Lebrasseur, J. F. Bean, E. Phillips, W. R. Frontera, and R. A. Fielding, "High-Intensity Resistance Training Improves Muscle," *Stroke*, vol. 35, pp. 1404–9, 2004.
- [8] M. Corti, T. E. McGuirk, S. S. Wu, and C. Patten, "Differential effects of power training versus functional task practice on compensation and restoration of arm function after stroke," *Neurorehabilitation and neural repair*, vol. 26, pp. 842–54, sep 2012.
- [9] L. Marchal-Crespo and D. J. Reinkensmeyer, "Review of control strategies for robotic movement training after neurologic injury," *Journal of neuroengineering and rehabilitation*, vol. 6, p. 20, jan 2009.
- [10] J.-c. Metzger, O. Lamberg, A. Califfi, D. Dinacci, C. Petrillo, P. Rossi, F. M. Conti, and R. Gassert, "Assessment-driven selection and adaptation of exercise difficulty in robot-assisted therapy : a pilot study with a hand rehabilitation robot," pp. 1–14, 2014.
- [11] G. Rosati, J. E. Bobrow, and D. J. Reinkensmeyer, "Compliant Control of Post-Stroke Rehabilitation Robots: Using Movement-Specific Models to Improve Controller Performance," *Proceedings of the Asme International Mechanical Engineering Congress and Exposition 2008*, Vol 2, pp. 167–174, 2009.
- [12] P. S. Lum, C. G. Burgar, P. C. Shor, M. Majumdar, and M. Van der Loos, "Robot-assisted movement training compared with conventional therapy techniques for the rehabilitation of upper-limb motor function after stroke," *Archives of Physical Medicine and Rehabilitation*, vol. 83, no. 7, pp. 952–959, 2002.
- [13] A. H. a. Stienen, E. E. G. Hekman, F. C. T. Van Der Helm, G. B. Prange, M. J. a. Jannink, A. M. M. Aalsma, and H. D. Van Kooij, "Dampace: Dynamic force-coordination trainer for the upper extremities," *2007 IEEE 10th International Conference on Rehabilitation Robotics, ICORR'07*, vol. 00, no. c, pp. 820–826, 2007.

- [14] M. F. Levin, R. W. Selles, M. H. G. Verheul, and O. G. Meijer, "Deficits in the coordination of agonist and antagonist muscles in stroke patients: implications for normal motor control.," *Brain research*, vol. 853, no. 2, pp. 352–369, 2000.
- [15] A. Philippou, G. C. Bogdanis, A. M. Nevill, and M. Maridaki, "Changes in the angle-force curve of human elbow flexors following eccentric and isometric exercise," *European Journal of Applied Physiology*, vol. 93, no. 1-2, pp. 237–244, 2004.
- [16] G. Alankus, A. Lazar, M. May, and C. Kelleher, "Towards customizable games for stroke rehabilitation," *Proceedings of the 28th international conference on Human factors in computing systems - CHI '10*, no. 2113, p. 2113, 2010.
- [17] M. Guidali, A. Duschau-Wicke, S. Broggi, V. Klamroth-Marganska, T. Nef, and R. Riener, "A robotic system to train activities of daily living in a virtual environment," *Medical and Biological Engineering and Computing*, vol. 49, pp. 1213–1223, oct 2011.
- [18] T. Nef, M. Mihelj, and R. Riener, "ARMin: a robot for patient-cooperative arm therapy.," *Medical & biological engineering & computing*, vol. 45, pp. 887–900, sep 2007.
- [19] U. Keller, S. Schölch, U. Albisser, C. Rudhe, A. Curt, R. Riener, and V. Klamroth-Marganska, "Robot-Assisted Arm Assessments in Spinal Cord Injured Patients: A Consideration of Concept Study," *Plos One*, vol. 10, no. 5, p. e0126948, 2015.
- [20] J. Lanini, T. Tsuji, P. Wolf, R. Riener, and D. Novak, "Teleoperation of two six-degree-of-freedom arm rehabilitation exoskeletons," in *ICORR International Conference on Rehabilitation Robotics*, 2015.
- [21] E. McAuley, T. Duncan, and V. V. Tammen, "Psychometric properties of the Intrinsic Motivation Inventory in a competitive sport setting: a confirmatory factor analysis.," 1989.
- [22] R. Colombo, F. Pisano, A. Mazzone, C. Delconte, S. Micera, M. C. Carrozza, P. Dario, and G. Minuco, "Design strategies to improve patient motivation during robot-aided rehabilitation.," *Journal of neuroengineering and rehabilitation*, vol. 4, p. 3, jan 2007.
- [23] M. Mihelj, D. Novak, M. Milavec, J. Zihlerl, A. Olenšek, and M. Murnih, "Virtual Rehabilitation Environment Using Principles of Intrinsic Motivation and Game Design," *Presence: Teleoperators and Virtual Environments*, vol. 21, pp. 1–15, feb 2012.
- [24] D. Novak, A. Nagle, U. Keller, and R. Riener, "Increasing motivation in robot-aided arm rehabilitation with competitive and cooperative gameplay.," *Journal of neuroengineering and rehabilitation*, vol. 11, no. 1, p. 64, 2014.